

## On the Catalytic Oxidation of Amorphous Carbon by Pd and Pd–Ag Particles

B. PENNEMANN<sup>1</sup> AND R. ANTON<sup>2</sup>

*Institut für Angewandte Physik, Universität Hamburg, Jungiusstr. 11, 2000 Hamburg 36, Federal Republic of Germany*

Received January 20, 1988; revised March 29, 1989

The catalytic oxidation of amorphous carbon by small Pd and Pd–Ag particles (15–20 nm in diameter) was investigated using a transmission electron microscope. The catalytic activities of the particles were measured by observation of the growth of holes oxidized into the carbon support films. The results show an increase of activity with growing size of the particles and increasing temperature and oxygen pressure. The highest activities were observed for pure Pd particles whereas pure Ag particles were completely inactive. Small concentrations of Ag reduced the activity drastically, compared with the expected value corresponding to the bulk composition. This is interpreted in terms of surface segregation and of the size of the site required for oxygen adsorption. © 1989 Academic Press, Inc.

### 1. INTRODUCTION

The catalytic oxidation of amorphous carbon and graphite by small Pd particles at temperatures of around 800 K and under pressures below 1 mbar is well known (see, for example, Refs. (1–4)). Some of these studies were performed in transmission electron microscopes, demonstrating the dramatic changes which the crystals and the support (substrate) undergo during the reaction (3, 4). However, our understanding of the reaction mechanism is still not very good. For example, it would be very valuable in such studies to determine the nature and size of the active sites. One possible way to obtain such information is to dilute the surface with an inactive material and measure the variations in activity. Also, the kinetics of the reaction should be investigated with the aim of determining the activation energy for the reaction.

<sup>1</sup> Present address: Institut für Physikalische und Theoretische Chemie, Universität Bonn, Wegelerstrasse 12, D-5300 Bonn 1, Federal Republic of Germany.

<sup>2</sup> To whom correspondence should be addressed.

### 2. EXPERIMENTAL

The studies were performed in a conventional TEM (Philips EM 400), equipped with a bakeable UHV chamber (Fig. 1) (5). The chamber was pumped by a turbomolecular pump (Balzers TPU 330) selected for minimum vibrations and was flanged with a damping bellows. It was checked that the modification of the microscope did not affect the resolution of 0.3 nm. The base pressure in the chamber with a filled liquid nitrogen cooling trap was  $8 \times 10^{-9}$  mbar, limited by backstreaming water vapor from the microscope column. The chamber contained two Knudsen-like evaporation cells and a gas inlet system. The chamber could be pressurized with O<sub>2</sub> (purity 99.995%) up to a pressure of  $10^{-5}$  mbar.

*In situ* electron microscopes built by other groups are usually said to have better vacuums at the site of the specimen (6, 7). One system encloses the sample in a cryocage, cooled with He, and gives an estimated base pressure in the  $10^{-10}$ -mbar range (7). The approach by Heinemann and Poppa (6) uses a fully bakeable minichamber, differentially pumped with an ion and a

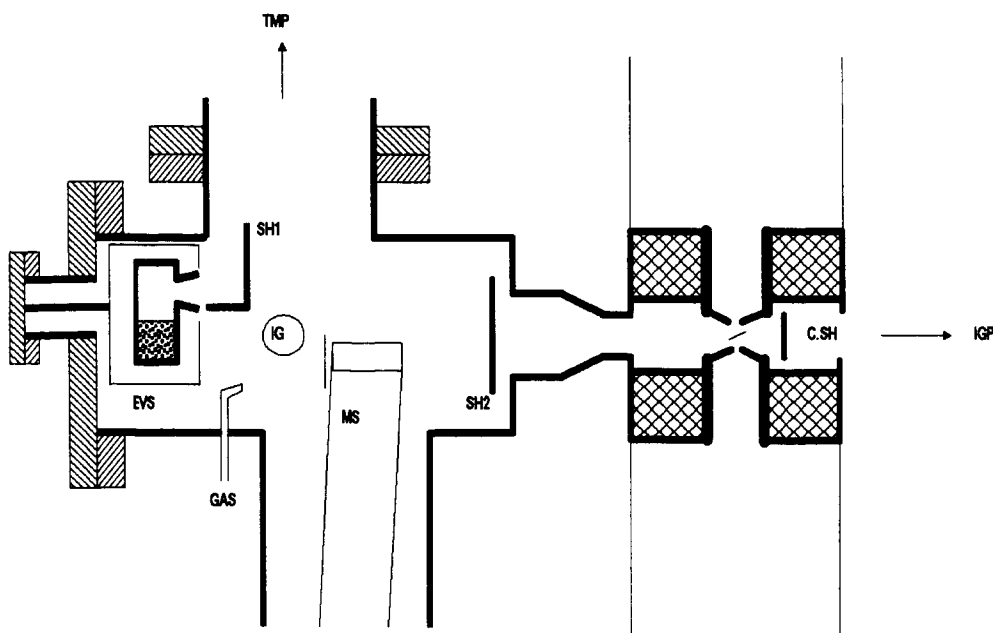


FIG. 1. Cross section of the chamber (left) as attached to the object stage of the microscope column (right). It contains two evaporator cells (EVS), ionization gauge (IG), gas inlet valve (GAS), quadrupole mass spectrometer (MS), and two shutters (SH1, SH2). The chamber is evacuated by a turbomolecular pump (TMP), whereas the column is pumped by an ion getter pump (IGP) and contains a cooling shield cooled with liquid nitrogen (C.SH).

sublimation pump to obtain similar pressures. However, a turbomolecular pump seems to be best suited for pumping the gas loads necessary for the experiments described.

Thin-film carbon substrates of 10- to 20-nm thickness were prepared *ex situ* in the following way: carbon was evaporated onto mica, floated off on water, picked up with Mo grids and mounted in the heatable TEM-specimen holder. After insertion into the microscope, the sample was heated to 1000 K for several hours, thereby removing the water embedded in the foil.

Pd or Ag was vapor-deposited *in situ* from the Knudsen cells at a rate of 0.05 nm/min until an average thickness between 0.7 and 2.0 nm was obtained; the particle sizes were between 15 and 20 nm.

The chamber was equipped with a quadrupole mass spectrometer, which was used for residual gas analysis as well as for monitoring the density and composition of the

evaporation beam and thus determining the amount and composition of the deposited metal. The signal of the mass spectrometer was calibrated for Pd and Ag independently using an X-ray fluorescence spectrometer. The composition of the deposit was also checked by measuring the lattice constant and by energy dispersive X-ray analysis in a SEM, using a special holder for low background, thus obtaining a detection limit of about  $5 \times 10^{-9}$  g/cm<sup>2</sup>.

### 3. RESULTS

The mean sizes and interparticle distances are highly influenced by the substrate temperature during evaporation (8), whereas annealing of samples prepared at room temperature causes only slight modifications. We applied substrate temperatures between 300 and 825 K. Here we shall only consider results obtained from samples at a substrate temperature of about 680 K during deposition. If the samples were exposed

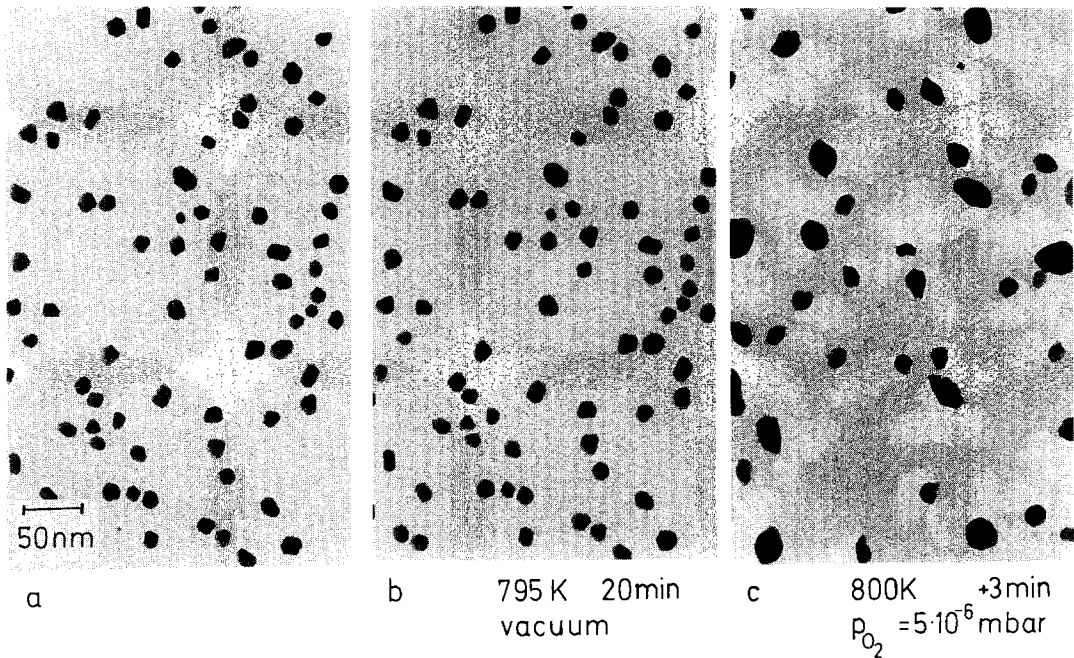


FIG. 2. Pd sample, deposited at 690 K with an average thickness of 1.7 nm. The sample is shown (a) as deposited, (b) after annealing at 795 K for 20 min under vacuum, and (c) after subsequent annealing for 3 min in  $5 \times 10^{-6}$  mbar  $O_2$ . Annealing under vacuum causes no changes, whereas annealing in  $O_2$  leads to a rapid gasification of the substrate.

to oxygen at around  $5 \times 10^{-6}$  mbar, the particles started to move across the substrate, thereby oxidizing it such that at first channels developed which grew to rather large holes (Fig. 2). During this process, the particles changed their shapes rapidly in a liquid-like fashion, although they always showed Bragg contrast and thus remained crystalline. After creating holes, the particles moved along the perimeter of their hole, still oxidizing the substrate. The speed of the particles was around 1 nm/s. In this way, the hole grew with time and the rate of its growth depended on the catalytic activity of the particle. The rate was determined from the photographs made after suitable time intervals, each displaying several particles used for the analysis.

An influence of the electron beam, as reported by Moorhead *et al.* (4), was never observed. The activity of particles irradiated by the beam during exposure to  $O_2$  was

carefully ascertained to be equal to that of other, nonirradiated particles. This difference may stem from our much thinner substrates (10 instead of 100 nm) which reduced the local thermal load due to the beam. In addition, the electron beam was only switched on intermittently for recording photographs in our experiments, and thus the total beam dosage was drastically reduced. This is important, because an increase in substrate temperature increases the activity of the particles, as shown below.

As is shown in Fig. 3, a linear relationship between the growth speed of the holes, expressed in oxidized C atoms per second, and the projected area of the corresponding particle holds. Thus, with the assumption of an almost constant shape of the particles, it seemed reasonable to interpret the following experiments in terms of a turnover rate. This assumption is supported by mea-

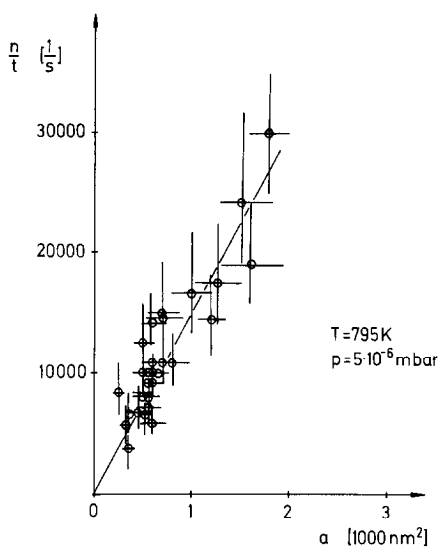


FIG. 3. Rate of oxidized substrate atoms ( $n/t$ ) as a function of the projected area of the oxidizing particle. Samples used were pure Pd. Substrate temperature was 795 K, and oxygen pressure was  $5 \times 10^{-6}$  mbar.

measurements of the projected area, which change less than 20% for a given particle during the reaction. The following measurements were therefore normalized to the size of the investigated particles.

Figure 4 shows the average activity of the particles as a function of the oxygen pressure. The data fit the expected linear relationship reasonably well. Due to the low activity and resulting small changes in hole size, measurements below  $5 \times 10^{-7}$  mbar are prone to errors. In addition, systematic deviations in the shape of the observed particles take place at these low pressures. The particles seem to flatten in shape and increase the surface area in contact with the substrate. This effect diminishes at higher pressures.

A similar effect was observed at higher temperatures (Fig. 5). At 950 K, the particles become thin and adopt the shape of the holes. The thickness falls steadily and, after more than 3 min, the particles start to rip into two pieces and each half continues to decrease in thickness. After reducing the

temperature, the particles shrink to their original, roughly spherical shape.

This effect necessarily influences the measured activity as a function of reciprocal temperature (Fig. 6) because this change of the shape of the particles increases their surface area. Also, the heat of reaction may lead to errors in this curve by increasing the temperature of the particles over that of the substrate by an unknown amount. Thus, the slope of the solid line in Fig. 6 should not be referred to as leading to an activation energy, although it is apparent that an activation barrier exists. In the regime of temperature below 700 K, the slope of the curve indicates an activation energy of  $65 \text{ kJ mol}^{-1}$ .

Figure 7 shows the activity of the samples, plotted against their bulk composition. Even at very low Ag contents, the catalytic activity of the samples is drastically reduced. Pure Ag particles were inactive under all accessible experimental conditions.

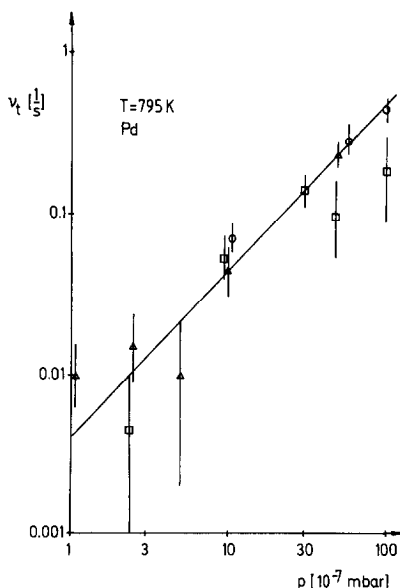
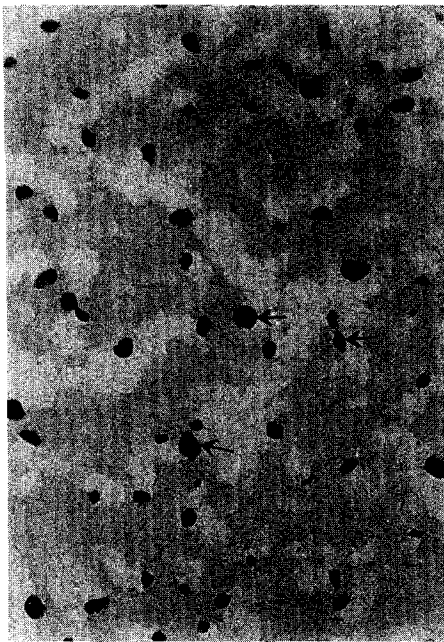
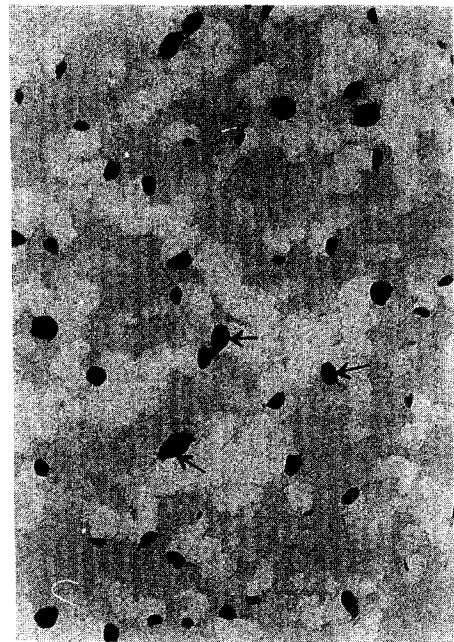


FIG. 4. Dependence of the turnover rate on the oxygen partial pressure. Each symbol corresponds to one sample. Under the assumption of a spherical shape of the particles, the scaling on the y-axis is the number of oxidation steps per surface atom and per second.



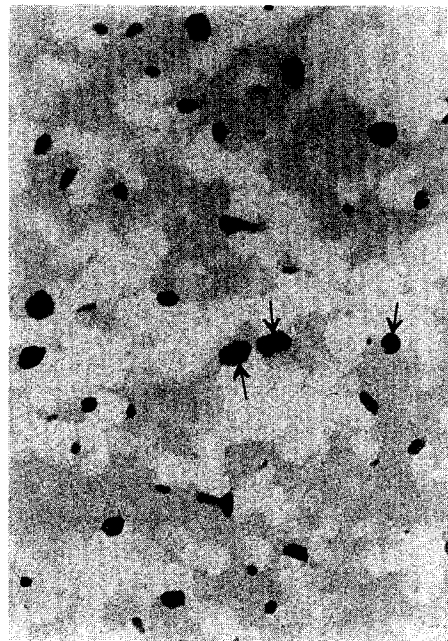
a 725K  
 $p_{O_2} = 5 \cdot 10^{-6} \text{ mbar}$



b 890K +3min



c 950K +3min



d 770K +3min

FIG. 5. Shape of the particles during oxygen exposure at various temperatures. At 890 K (b) and especially at 950 K (c) the particles become thin and flat, wetting the substrate foil. This is reversible, as shown in (d), where the particles obtain shapes almost similar to those in (a). Three individual particles were marked with arrows.

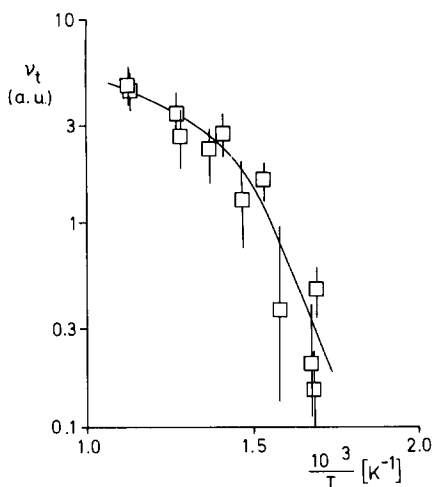


Fig. 6. Catalytic activity (in arbitrary units) as a function of reciprocal temperature. The slope on the low-temperature side of the curve is estimated to be equivalent to an activation energy of  $65 \text{ kJ mol}^{-1}$ .

#### 4. DISCUSSION

Although our result of an activation energy is only an estimate, the value of  $65 \text{ kJ mol}^{-1}$  at and below  $700 \text{ K}$  was compared with data for Pd and Ag as given by Heintz and Parker (1). They have investigated the oxidation of graphite, catalyzed by metal powder, in air, under atmospheric pressure, and at temperatures well above  $850 \text{ K}$ . At  $873 \text{ K}$ , their measured oxidation rates were higher with Ag by about four to five times than with Pd; but at  $973 \text{ K}$ , the rate with Pd was increased by 150 times, whereas that with Ag was decreased to 0.2 of its value at the lower temperature. In contrast, the authors found activation energies of  $520 \text{ kJ mol}^{-1}$  for Pd, and  $47 \text{ kJ mol}^{-1}$  for Ag. They argued that this unusual behavior can be explained by an opposite trend of the preexponentials, probably due to a change in the active surface area. It seems that this behavior cannot easily be extrapolated to our conditions of lower temperatures and much lower pressures. As was indicated by our observations of changes of the particle shapes under low oxygen partial pressures as well as at high temperatures, changes in

the active surface area or dispersion of the material can be expected at even higher temperatures.

Comparison was also made with independent determinations of the surface composition of Pd–Ag alloys. Kuijers and Ponc (9) investigated Pd–Ag catalysts by Auger electron spectroscopy. They found a strong enrichment of Ag in the surface when the samples were annealed for several hours at elevated temperature, which is also expected for thermodynamic reasons. Their data of the surface content of Pd as a function of the bulk composition is also plotted in Fig. 7 for comparison. These findings were supported by CO adsorption studies from Nordmeer *et al.* (10). The authors also dealt with the problem of surface order. Their Monte Carlo calculations showed that the surface and bulk distributions of both kinds of atoms should be random. The perfect miscibility of Pd and Ag gives another indication of a random distribution. Such distributions are rather difficult to measure, but experimental evidence from

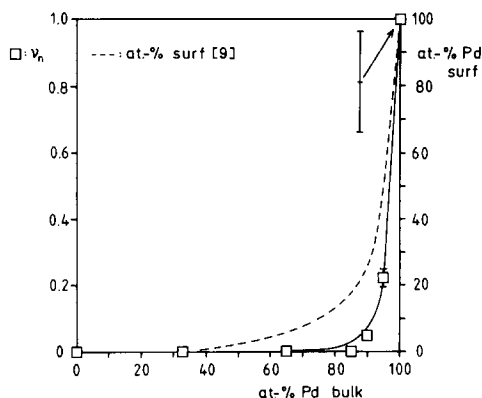


Fig. 7. Catalytic activity (left-hand scale) vs the bulk composition of the particles. The dashed curve shows the surface concentration of Pd (right-hand scale) as a function of bulk composition, as measured by Kuijers and Ponc (9). The full curve corresponds to the square of the surface concentration, thus showing that the activity is proportional to the square of the density of Pd atoms at the surface. All data were obtained at a substrate temperature of  $795 \text{ K}$  and under an  $\text{O}_2$  partial pressure of  $5 \times 10^{-6} \text{ mbar}$ .

CO adsorption studies seems to support this view. An overview of these experiments has been given by Nieuwenhuys (11).

At this point, it is interesting to calculate the thickness of a segregated layer of Ag as a function of the particle size and composition under the assumption that all of the Ag would be present at the surface, thus forming a shell around a core of Pd. The result is that at an integrated (bulk) concentration of 0.15 of Ag (corresponding to 85 mol% Pd) the particle surface would be pure Ag for sizes above 5 nm. In fact, at this composition, our particles with sizes from 15 to 20 nm were inactive, as was pure Ag. However, this extreme case does not appear to be reasonable, as the Monte Carlo calculations mentioned above indicate. Therefore we used the curve from Kuijers and Ponec to estimate the surface composition of our particles. Figure 7 shows that the activity is not proportional to the surface composition, but decreases faster with decreasing Pd content. Instead, the measured activity is well fitted by the square of the Pd surface concentration. Thus it seems reasonable to assume that two adjacent Pd atoms are required for the dissociative adsorption of O<sub>2</sub> (see also Ref. (12)), whereas no oxygen is adsorbed on Ag at the substrate temperatures applied in our experiments.

This agrees well with thermal desorption spectra experiments of dissociatively adsorbed O<sub>2</sub> on close-packed Ag surfaces which exhibit a very low sticking coefficient and a desorption maximum at about 600 K (13, 14), which is at the lower end of our temperature range. The desorption maximum from Pd surfaces is around 800 K (15, 16), a temperature at which the slope of the measured activity deviates remarkably from a straight line. This could be ascribed to a reduced sticking probability of O<sub>2</sub> at these temperatures.

In the same way the observed flattening of the Pd particles at higher temperatures may stem from a reduced oxygen coverage, similar to our observations at low pressures.

An influence of changes in the electronic structure of the Pd atoms due to alloying (ligand effect) on the observed dependence of activity vs bulk composition should be of minor importance. Independent investigations of surface segregation under such conditions are needed to clarify the situation.

#### REFERENCES

1. Heintz, E. A., and Parker, W. E., *Carbon* **4**, 473 (1966).
2. Fryer, J. R., *Nature (London)* **220**, 1121 (1968).
3. Anton, R., and Poppa, H., in "Proceedings, 10th Intern. Congr. Electron Microscopy, Hamburg, 1982," p. 509. Deutsche Gesellschaft für Elektronenmikroskopie, Frankfurt, 1982.
4. Moorhead, R. D., Poppa, H., and Heinemann, K., *J. Vac. Sci. Technol.* **17**(1), 248 (1980).
5. Anton, R., *J. Electron Microsc. Suppl.* **35.1**, 339 (1986).
6. Heinemann, K., and Poppa, H., *J. Vac. Sci. Technol. A* **4**(1), 127 (1986).
7. Takayanagi, K., Yagi, K., Kobayashi, K., and Honjo, G., *J. Phys. E* **11**, 441 (1978).
8. Anton, R., in "Studies in Surface Science and Catalysis" (P. Wissmann, Ed.), Vol. 32, p. 1. Elsevier, Amsterdam/New York, 1987.
9. Kuijers, F. J., and Ponec, V., *J. Catal.* **60**, 100 (1979).
10. Nordmeer, A., Kok, G. A., and Nieuwenhuys, B. E., *Surf. Sci.* **165**, 375 (1986).
11. Nieuwenhuys, B. E., in "Studies in Surface Science and Catalysis (P. Wissmann, Ed.), Vol. 32, p. 476. Elsevier, Amsterdam/New York, 1987.
12. Doering, D. L., Poppa, H., and Dickinson, J. T., *J. Catal.* **73**, 104 (1981).
13. Campbell, C. T., *Surf. Sci.* **157**, 43 (1985).
14. Bao, X., Deng, J., and Dong, Sh., *Surf. Sci.* **163**, 444 (1985).
15. Stuve, E. M., Madix, R. J., and Brundle, C. R., *Surf. Sci.* **146**, 155 (1984).
16. Weissmann, D. L., Shek, M. L., and Spicer, W. E., *Surf. Sci.* **92**, L59 (1980).